Biology of Reproduction, 2021, 104(6), 1218–1227
doi:10.1093/biolre/ioab031
Research Article
Advance Access Publication Date: 4 March 2021

OXFORD

Research Article

Time-lapse imaging of human embryos fertilized with testicular sperm reveals an impact on the first embryonic cell cycle

E.S. van Marion[1,*], J.P. Speksnijder[1], J. Hoek[2], W.P.A. Boellaard[3], M. Dinkelman-Smit[3], E.A. Chavli[1], R.P.M. Steegers-Theunissen[2], J.S.E. Laven[1] and E.B. Baart[1,4]

[1]Division of Reproductive Endocrinology and Infertility, Department of Obstetrics and Gynaecology, Erasmus MC, University Medical Center, Rotterdam, The Netherlands, [2]Department of Obstetrics and Gynaecology, Erasmus MC, University Medical Center, Rotterdam, The Netherlands, [3]Department of Urology, Erasmus MC, University Medical Center, Rotterdam, The Netherlands and [4]Department of Developmental Biology, Erasmus MC, University Medical Center, Rotterdam, The Netherlands

***Correspondence:** Division of Reproductive Endocrinology and Infertility, Department of Obstetrics and Gynaecology; Erasmus MC, University Medical Center, Rotterdam, PO Box 2040, 3000 CA Rotterdam, the Netherlands. Tel: +31629199006; E-mail: e.vanmarion@erasmusmc.nl

Received 24 December 2020; Revised 8 February 2021; Accepted 18 February 2021

Abstract

Testicular sperm is increasingly used during in vitro fertilization treatment. Testicular sperm has the ability to fertilize the oocyte after intracytoplasmic sperm injection (ICSI), but they have not undergone maturation during epididymal transport. Testicular sperm differs from ejaculated sperm in terms of chromatin maturity, incidence of DNA damage, and RNA content. It is not fully understood what the biological impact is of using testicular sperm, on fertilization, preimplantation embryo development, and postimplantation development. Our goal was to investigate differences in human preimplantation embryo development after ICSI using testicular sperm (TESE-ICSI) and ejaculated sperm. We used time-lapse embryo culture to study these possible differences. Embryos (n = 639) originating from 208 couples undergoing TESE-ICSI treatment were studied and compared to embryos (n = 866) originating from 243 couples undergoing ICSI treatment with ejaculated sperm. Using statistical analysis with linear mixed models, we observed that pronuclei appeared 0.55 h earlier in TESE-ICSI embryos, after which the pronuclear stage lasted 0.55 h longer. Also, significantly more TESE-ICSI embryos showed direct unequal cleavage from the 1-cell stage to the 3-cell stage. TESE-ICSI embryos proceeded faster through the cleavage divisions to the 5- and the 6-cell stage, but this effect disappeared when we adjusted our model for maternal factors. In conclusion, sperm origin affects embryo development during the first embryonic cell cycle, but not developmental kinetics to the 8-cell stage. Our results provide insight into the biological differences between testicular and ejaculated sperm and their impact during human fertilization.

Summary sentence

Human embryos originating from fertilization with testicular sperm show a prolonged pronuclear stage and more often direct unequal cleavage than embryos originating from ejaculated sperm, while subsequent cleavage divisions are not impacted.

Key words: preimplantation embryo development, intracytoplasmic sperm injections, fertilization in vitro, infertility, testicular spermatozoa, time-lapse imaging, gamete biology, sperm maturation, assisted reproductive technology.

Introduction

Since the discovery of testicular sperm extraction (TESE), it became possible for men with azoospermia to have offspring through in vitro fertilization (IVF) with intracytoplasmic sperm injection (ICSI) [1–4]. In patients diagnosed with nonobstructive azoospermia (NOA), TESE is the treatment of choice [5–7]. TESE can also be performed in the case of postvasectomy, iatrogenic, congenital, or postinfectious obstructive azoospermia (OA), or when vasovasostomy or microsurgical epididymal sperm aspiration (MESA) failed [8].

Initially, there were concerns on the safety of using testicular-derived sperm for IVF treatment. Higher rates of aneuploidy and chromosomal mosaicism have been reported in human embryos originating from fertilization with testicular sperm [9, 10]. However, TESE-ICSI has become a widely used treatment, with similar pregnancy and live birth rates reported as after treatment cycles with ejaculated sperm [11]. Still, biological differences exist between testicular and ejaculated spermatozoa. Testicular spermatozoa can be fully formed, but have not yet acquired progressive motility [12]. When used for ICSI treatment, they do have the ability to activate and fertilize the oocyte [3, 13–15]. However, important changes in sperm maturity occur during epididymal transit, where forward motility is acquired and sperm chromatin condensation increases [12, 16, 17]. Surgically retrieved testicular spermatozoa have not undergone these final steps of maturation during transport through the male reproductive tract. Interestingly, a lower sperm DNA fragmentation (SDF) index has been reported in testicular spermatozoa than in ejaculated spermatozoa [18]. This evidence suggests that the level of DNA damage in sperm may increase during epididymal transit. Moreover, during ejaculation, spermatozoa normally come into contact with additional fluids from the seminal vesicle and prostate. Accumulating evidence indicates that membrane bound extracellular vesicles called exosomes are present in these additional fluids. These exosomes contain both coding and small noncoding RNAs that are added to the sperm with potential roles in embryo development [19].

Furthermore, at the onset of meiosis, the formation and repair of DNA double-strand breaks is an essential feature of meiotic recombination. After the completion of male meiosis and during subsequent spermiogenesis, histones enfolding the DNA are almost completely replaced by protamines, and this major chromatin remodeling process is again accompanied by a transient increase in single- and double-strand DNA breaks [20]. Concomitant with the remodeling process, the capacity of spermatids to repair DNA breaks progressively declines [21, 22]. As a consequence, residual DNA damage from spermatogenesis or novel damage acquired during transport through the reproductive tract remains to be repaired in the oocyte after fertilization [23, 24]. After fertilization, the sperm chromatin again undergoes extensive remodeling, as protamines are replaced by histones [25, 26]. As sperm chromatin is still undergoing further condensation during transit from the testis to the epididymis, chromatin compaction differences may exist between testicular and ejaculated spermatozoa that may also impact the protamine-to-histone transition after fertilization.

Overall, human testicular spermatozoa differ from ejaculated spermatozoa in terms of chromatin maturity, incidence of DNA damage, and RNA content. It is unclear what the impact is of these differences on fertilization, preimplantation embryo development and development after implantation. Time-lapse embryo culture is a noninvasive tool to study preimplantation embryo development, as it provides an uninterrupted controlled culture environment while capturing the timing of each developmental stage of the preimplantation embryo. Developmental time points, referred to as morphokinetic parameters, are shown to be associated with maternal characteristics such as smoking and bodyweight, culture conditions such as oxygen concentration and type of culture medium, as well as treatment-related factors such as fertilization method and ovarian stimulation regimen [27–33]. Earlier studies compared small groups of TESE-ICSI embryos with ICSI embryos originating from ejaculated sperm, and conflicting results were reported on the impact on the timings of the cleavage divisions [34–38]. However, it is shown that embryos originating from one patient share a comparable developmental timing, which is called clustering [39]. In these former studies, clustering of embryos originating from one patient was not taken into account, introducing a potential bias by a large amount of embryos originating from the same patients. It is therefore inconclusive what the impact of using testicular sperm for fertilization is on the cleavage divisions of human embryos.

A recent study showed that placental growth trajectories in the first trimester of pregnancy are increased in pregnancies conceived after TESE-ICSI as compared to ICSI with ejaculated sperm [40]. To better understand the origin of these biological differences in postimplantation embryo development resulting from ICSI with testicular and ejaculated sperm, we investigated a larger cohort of TESE-ICSI preimplantation embryos using time-lapse culture, and compared their developmental kinetics during the cleavage divisions with ICSI embryos originating from ejaculated sperm.

Materials and methods

Study design and participants

We retrospectively analyzed data from couples undergoing a TESE-ICSI cycle or an ICSI cycle with ejaculated sperm in combination with time-lapse embryo culture at the Erasmus MC, University Medical Center between 2014 and 2019. TESE-ICSI indications were NOA or postvasectomy, iatrogenic, congenital or postinfectious OA. TESE-ICSI was also performed when vasovasostomy or MESA had failed and in some cases for cryptozoospermia. Indications for ICSI with ejaculated sperm were male factor infertility or a previous IVF cycle resulting in total fertilization failure (TFF). Only cycles with autologous, fresh oocytes were included. From couples undergoing multiple cycles during the study period, only data from their first available treatment cycle was included.

Testicular sperm retrieval, testicular, and ejaculated sperm processing

Testicular sperm extraction was performed under local anesthesia with a standard open surgical biopsy technique. A transverse 2 centimeter (cm) scrotal incision was made. The tunica albuginea was incised for 1 cm and a small fragment (approximately 1.5 cm^3) of testicular tissue was excised with sharp scissors and placed in

SAGE HEPES buffered human tubal fluid (HTF) culture medium supplemented with 5% (w/v) human serum albumin (HSA) (all from Origio/Cooper Surgical, Trumbull, CT, USA). Testicular tissue consisting of tubuli seminifiri was dissected using sterile glass slides, and the resulting spermatogenic cell suspension was washed with HTF, followed by centrifugation at 900 g for 10 min. The pellet was resuspended in 1 milliliter (ml) HTF and subsequently diluted 1:1 with cryoprotectant (Test Yolk Buffer, Irvine Scientific, Santa Ana, USA) and cryopreserved in straws (Cryo Bio System, Saint-Ouen-sur-Iton, France) by placing them in liquid nitrogen vapor.

Before use, testicular sperm cells were thawed and washed with 5 ml HTF supplemented with 10% HSA and centrifuged at 670 g for 5 min. The remaining pellet was resuspended in 1 ml HTF/10% HSA and carefully layered on top of 1 ml 40% PureSperm and centrifuged at 670 g for 30 min. The upper layer of the gradient was removed, leaving only the soft pellet. This was washed in 5 ml HTF and stored at 37°C for a minimum of 1.5 h. An ICSI dish was prepared containing 75 microliters (µl) drops of HTF under liquid paraffin oil (Origio), and the purified spermatogenic cells were pipetted into the drops. Best quality sperm cells, according to motility and morphology, were selected under an inverted microscope (Leica microsystems, Germany) at 200–400 times magnification.

Ejaculated semen samples were left to liquefy and sperm concentration and motility were determined. They were subsequently processed by density centrifugation, using a 40–80% PureSperm density gradient (Nidacon International AB, Mölndal, Sweden) according to the manufacturer's instructions. The resulting soft pellet was washed twice in HTF medium and isolated spermatozoa were stored at room temperature until the ICSI procedure. Sperm samples were classified according to concentration and motility into samples showing oligo- or normozoospermia, and samples showing severe oligoasthenozoospermia, where all quality parameters are below the lower reference limits as defined by the World Health Organization laboratory manual [41]. Severe oligoasthenozoospermia was defined as: volume x concentration x percentage progressively motile spermatozoa/100 is less than 1 million.

Ovarian stimulation, oocyte collection and oocyte injection

Women underwent routine ovarian stimulation by either a GnRH-agonist or -antagonist co-treatment protocol with recombinant- or urinary- follicle stimulating hormone (FSH; Bemfola, Gedeon Richter, Belgium, Menopur, Ferring, St. Prex, Switzerland, Gonal-F, Merck Serono, Switzerland or Rekovelle, Ferring, St. Prex, Switzerland) [42]. Ovarian stimulation protocols are standardized at our center and the distribution of GnRH-agonist or antagonist protocol reflects policy changes over time and not patient selection. Human recombinant chorionic gonadotropin (hCG) (Pregnyl, Organon, the Netherlands) was used as a trigger of final follicular maturation. Ovum pick up was planned according to standardized criteria. For ICSI with ejaculated sperm, metaphase II (MII) oocytes were injected with motile ejaculated spermatozoa. For ICSI with testicular sperm, MII oocytes were injected with either motile testicular spermatozoa or immotile but viable testicular spermatozoa, as selected by a sperm tail flexibility test [43].

Embryo culture, selection, and transfer

Injected oocytes were placed in individual wells of EmbryoSlide culture dishes (Vitrolife, Göteborg, Sweden) and were cultured in an EmbryoScope time-lapse incubator (Vitrolife, Göteborg, Sweden) in SAGE 1-Step medium (Origio/Cooper Surgical) at 36.8°C, 7% O_2 and 5% CO_2. Embryo transfer was performed on day 3 after fertilization until April 1, 2019. After this, because of a change in laboratory policy, embryo transfer was performed on day 5 after fertilization, concerning 26 treatment cycles included in this cohort. In our clinic, it is standard care to perform single embryo transfer (SET). Only women aged 38 years or older without medical contra-indications or women undergoing their third or higher treatment cycle can opt for double embryo transfer. Embryo selection for transfer was not aided by time-lapse information and was performed on a single image acquired by the EmbryoScope at 66–68 h postinjection. As implantation and pregnancy outcome were not primary outcomes in this study, this does not impact on our findings. Embryo morphology was ranked according to the number of blastomeres, fragmentation, equality of blastomere size, and cell contact. Top ranking embryos contained eight blastomeres of equal size, with less than 10% fragmentation. Embryo selection for cryopreservation was performed on a single image acquired by the EmbryoScope at 90–92 h postinjection. Embryos with at least 13 blastomeres or at least 30% compaction were cryopreserved [44]. For the 26 transfers, where embryo selection was performed on day 5, this was based on a single image at 114–116 h postinjection, and blastocysts were ranked by evaluating expansion, inner cell mass development, and trophectoderm appearance using the European Society of Human Reproduction and Embryology grading system [45]. Biochemical pregnancy was confirmed by a positive β-hCG test, ongoing pregnancy was confirmed by a fetal heartbeat during ultrasound at 12 weeks of gestation.

Time-lapse imaging and assessment

The EmbryoScope (Vitrolife) records images automatically in seven focal planes every 10 min. For both TESE-ICSI and ICSI with ejaculated sperm, $t = 0$ was defined as the time of injection of the last oocyte, with the whole procedure taking between 20–50 min, depending on the number of oocytes. Manual annotations were performed by four trained members of our team according to published consensus definitions and guidelines [46]. The time of pronuclear appearance (tPNa), number of pronuclei (PN), the first frame where both pronuclei faded (tPNf), the timing of reaching the 2-, 3-, 4-, 5-, 6-, 7-, and 8-cell stage (t2, t3, t4, t5, t6, t7, and t8; Figure 1). We tested the inter-observer agreement for annotations and found excellent agreement (intraclass correlation coefficient (ICC) > 0.9) for tPNa, tPNf and the cleavage divisions up until the 5-cell stage. Moderate agreement (ICC < 0.5) was found for the cleavage divisions between the 6- and the 8-cell stage.

We calculated the interval between pronuclear appearance and disappearance (tPNa-tPNf) and the interval between the 2-cell stage and the 3-cell stage (t3-t2) (Figure 1). Embryos were defined as direct unequal cleaving (DUC) if they needed 5 h or less during t3-t2 (Figure 2) [47].

Statistical analysis

Baseline data were tested for the assumption of normality. If continuous data did not fulfill the assumption of normality, a Mann–Whitney U test was performed and estimates are reported as medians and interquartile range (IQR). Categorical data were analyzed with the Chi-square test/Fisher exact test. Time-lapse data were analyzed using a linear mixed model to adjust for the issue that the developmental time points of one embryo cannot be considered as independent measurements and that embryos originating from one

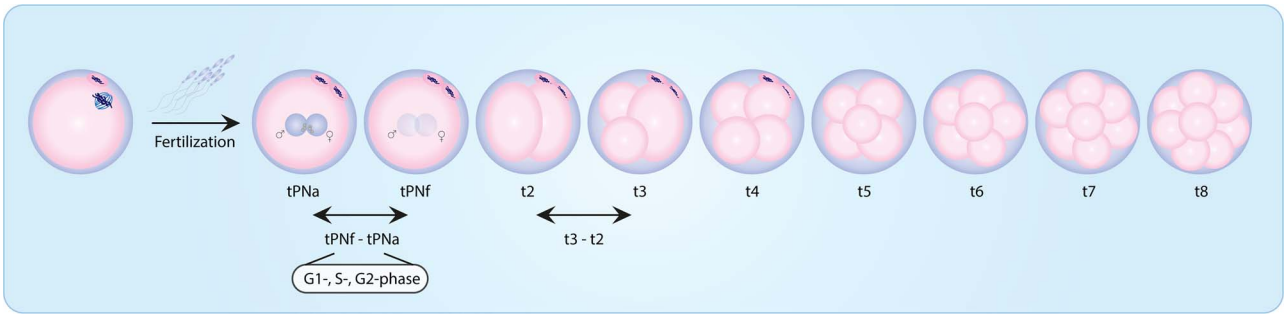

Figure 1. Schematic representation of embryo developmental events after fertilization. The morphokinetic events annotated in this study are indicated, as are the time intervals we calculated and used. Phases during the first embryonic cell cycle are also illustrated. G1-phase, gap 1 phase; S-phase, synthesis phase; G2-phase, gap 2 phase; tPNa, time interval between the time of injection of spermatozoa into the oocyte and appearance of the two pronuclei (PN); tPNf, fading of the PN; tPNf-tPNa, time interval between tPNa and tPNf; t2, time of cleavage of the embryo to the 2-cell stage; t3, time of cleavage of the embryo to the 3-cell stage; t3-t2, time interval between t2 and t3; t4, time of cleavage of the embryo to the 4-cell stage; t5, time of cleavage of the embryo to the 5-cell stage; t6, time of cleavage of the embryo to the 6-cell stage; t7, time of cleavage of the embryo to the 7-cell stage; t8, time of cleavage of the embryo to the 8-cell stage.

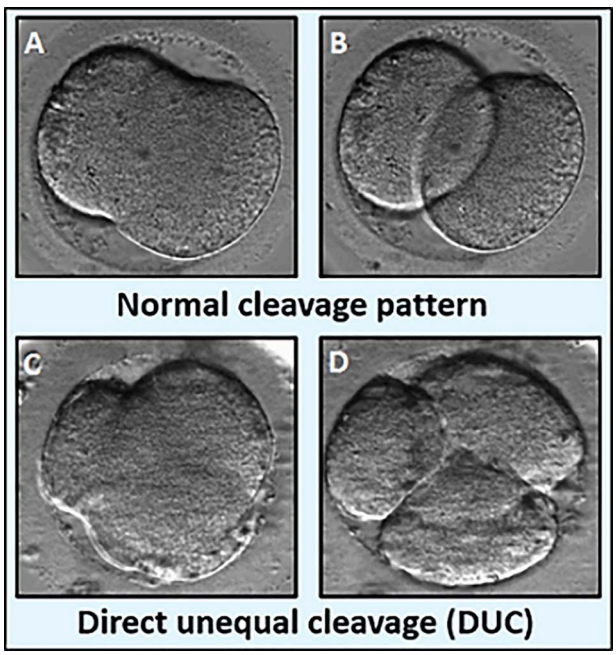

Figure 2. Representative images of human zygotes cultured in a time-lapse incubator undergoing the first cleavage division following a normal cleavage pattern (A, B) and direct unequal cleavage (C,D). Embryos were defined as direct unequal cleaving (DUC) if they needed 5 h or less during the interval between the 2- and the 3-cell stage.

couple show clustering [39]. All statistical analyses were performed in the statistical package for the social sciences (SPSS), version 24. Two-sided p-values < 0.05 were considered significant.

Ethical approval

The Medical Ethical Committee of the Erasmus MC examined the study protocol and issued a waiver for the Medical Research Act (in Dutch: Wet medisch-wetenschappelijk onderzoek met mensen (WMO)) (MEC-2016-041), so no formal consent was needed. All patients undergoing treatment at our center are informed that anonymized data may be used for retrospective research and patients have the opportunity to object to this. Patients that objected were excluded from the analysis.

Results

Patient characteristics and treatment outcome

We analyzed a total of 451 IVF-ICSI cycles, of which 208 TESE-ICSI cycles and 243 ICSI cycles with ejaculated sperm. Female and male age did not differ between the TESE-ICSI group and ICSI with ejaculated sperm group, with a median age of 33 years (IQR 29–36 and IQR 30–37) for women and 35 years (IQR 31–40 and IQR 31–41) for men. The type of ovarian stimulation regimen used was significantly different between the two groups (74% underwent GnRH-agonist co-treatment in the TESE-ICSI group vs 51% in the ICSI with ejaculated sperm group). The number of aspirated oocytes was significantly higher in the TESE-ICSI group with a median of 9 (IQR 6–14) oocytes and 7 (IQR 5–10) oocytes in the ICSI with ejaculated sperm group. Of the men who underwent TESE, 141 (67.8%) were diagnosed with NOA and 62 (29.8%) with OA, 5 (2.4%) were diagnosed with cryptozoospermia. Male factor infertility was diagnosed in 228 patients of the ICSI group with ejaculated sperm. The remaining 15 ICSI with ejaculated sperm cycles were performed because of a previous IVF cycle resulting in TFF. Treatment outcome characteristics of fresh embryo transfers are shown in Table 1. Fertilization rates were lower after TESE-ICSI, but no differences were observed in the proportion of fertilized oocytes resulting in an embryo used for transfer or cryopreservation. Pregnancy outcomes were also not different between the two groups. Within the TESE-ICSI group, cycles of men diagnosed with NOA resulted in a lower fertilization rate per oocyte retrieved than cycles of men diagnosed with OA (NOA 20.6% in the highest quartile of fertilization rate vs OA 30.6%, Supplementary Table S2). This is consistent with previous reports [48–50].

Embryo developmental kinetics

Representative time-lapse videos from embryos resulting after ICSI with testicular or ejaculated sperm were uploaded (Supplementary Videos S1 and S2). Embryos used for either fresh transfer or cryopreservation were annotated for tPNa, tPNf, and t2 up until t8 (Supplementary Table S1). The median times in hours needed to reach a certain developmental time point are presented (Table 2). In order to investigate differences in morphokinetics, we performed a linear mixed model analysis with ICSI embryos originating from ejaculated sperm as a reference, while taking clustering of embryos from each couple into account (Table 2, model 1). In a second

Table 1. Outcome characteristics of cycles included in the time-lapse analysis and pregnancy outcome after fresh embryo transfer in TESE-ICSI and ICSI with ejaculated sperm.

	TESE-ICSI	ICSI (with ejaculated sperm)	p-value
Number of analyzed cycles	208	243	
MII oocytes	7 (5–11)	6 (4–9)	<0.001
Fertilized oocytes	4 (2–6)	4 (2–6)	0.301
Fertilization rate (fertilized oocytes/MII oocytes)			
0–25%	30 (14.4)	10 (4.1)	<0.001
25.01–50%	55 (26.4)	39 (16.0)	
50.01–75%	73 (35.1)	79 (32.5)	
75.01–100%	50 (24.0)	115 (47.3)	
Total number of analyzed embryos	639	866	NA
Transferred	193 (30.2)	259 (29.9)	
Frozen	446 (69.8)	607 (70.1)	
Embryo usage rate (number of cryopreserved and transferred embryos/number of bi-pronuclear zygotes)			
0–25%	8 (3.8)	3 (1.2)	0.275
25.01–50%	50 (24.0)	60 (24.7)	
50.01–75%	46 (22.1)	64 (26.3)	
75.01–100%	102 (49.0)	116 (47.7)	
No bi-pronuclear zygotes	2 (1.0)	0 (0)	
Quality of injected testicular spermatozoa			NA
Motile spermatozoa	589 (92.2)	NA	
Immotile viable spermatozoa	50 (7.8)	NA	
Embryos transferred			
Single embryo transfer	175 (84.1)	195 (80.2)	0.001
Double embryo transfer	8 (3.8)	32 (13.2)	
No transfer	25 (12.0)	16 (6.6)	
Biochemical pregnancy (%)	82 (44.8)	102 (44.9)	0.980
Fetal heartbeat at 12 weeks of gestation (%)			
1	67 (36.6)	81 (35.7)	0.966
2	1 (0.5)	2 (0.9)	
	Live birth (%)		
Singleton	52 (28.4)	60 (26.4)	0.692
Twin	0 (0)	2 (0.9)	
Still pregnant during analysis	11 (6.0)	13 (5.7)	

Each cycle is derived from a unique patient couple. Data are presented as number (%) or median (interquartile range). A p-value of < 0.05 was considered significant. TESE-ICSI, testicular sperm extraction with intracytoplasmic sperm injection; ICSI, intracytoplasmic sperm injection; NA, not applicable; MII oocytes, metaphase II oocytes.

model, we also adjusted for the ovarian stimulation regimen with GnRH-agonist or -antagonist co-treatment (Table 2, model 2). Linear mixed model analysis showed a negative beta of 0.55 h for the start of tPNa. This means that tPNa started 0.55 h earlier in TESE-ICSI embryos compared to ICSI embryos originating from ejaculated sperm (95% confidence interval (CI): −0.85 to −0.25). Also, in TESE-ICSI embryos the interval from tPNa to tPNf was extended with 0.55 h (95% CI: 0.05 to 1.04) (Table 2, model 2).

After this initial delay, TESE-ICSI embryos reached the 5- and 6-cell stage 1.11 and 1.04 h earlier (95% CI: −2.16 to −0.05 and 95% CI: −2.06 to −0.03) than ICSI embryos originating from ejaculated sperm, but this effect disappeared after adjusting for the ovarian stimulation regimen (Table 2, models 1 and 2). We initially observed a significant difference in the time needed for the t3–t2 interval between TESE-ICSI and ICSI embryos originating from ejaculated sperm. However, in-depth analysis showed that significantly more TESE-ICSI embryos displayed DUC than ICSI embryos originating from ejaculated sperm (20.5% vs 13.6% respectively; p-value < 0.001), proceeding from the 2- to the 3-cell stage in 5 h or less (Table 3 and Supplementary Video S3). After exclusion of all DUC embryos from both groups, we did not observe a difference in timing of the interval t3–t2 in our linear mixed model analysis (data not shown). No significant difference in the occurrence of DUC was found in the TESE-ICSI group between the diagnosis NOA and OA (data not shown). In our cohort, embryo selection for transfer was not based on time-lapse information, so 45 DUC embryos were unknowingly selected for SET based on their morphology on the day of transfer. The transfer of DUC embryos resulted in a lower live birth rate than normal cleaving embryos (8.9% for DUC embryos vs 30.5% for normal cleaving embryos; p-value 0.001; Table 3) irrespective of sperm origin.

When we compared TESE-ICSI embryos originating from men with a diagnosis of NOA (434 embryos) or OA (190 embryos), we observed no differences in morphokinetics, except for an even faster pronuclear appearance for embryos originating from men with diagnosis NOA (beta −0.51 h 95% CI: −1.00 to −0.02) (Supplementary Table S3, model 2). The comparison of TESE-ICSI embryos derived from motile or immotile viable spermatozoa showed no significant differences in time-lapse morphokinetics (data not shown). When we stratified within the group of ICSI with ejaculated sperm for cycles with or without severe oligoasthenozoospermia, we found no significant differences in time-lapse morphokinetics (Supplementary Table S4).

Table 2. Results of the linear mixed model analysis comparing morphokinetic parameters from all transferred and cryopreserved embryos resulting from intracytoplasmic sperm injection with testicular sperm (TESE-ICSI), using embryos resulting after ICSI with ejaculated sperm as a reference

Morphokinetic parameters	Median (IQR) hours		Model 1 Beta [95% CI] hours			Model 2 Beta [95% CI] hours		
	TESE-ICSI	ICSI (ejaculated sperm)	TESE-ICSI	ICSI (ejaculated sperm)	p-value	TESE-ICSI	ICSI (ejaculated sperm)	p-value
tPNa	7.2 (6.1–8.7)	7.7 (6.7–9.1)	−0.49 [−0.78 to −0.20]	Reference	0.001	−0.55 [−0.85 to −0.25]	Reference	<0.001
tPNf	23.2 (21.4–25.3)	23.5 (21.6–25.3)	−0.06 [−0.56 to 0.43]	Reference	0.799	−0.01 [−0.52 to 0.51]	Reference	0.978
tPNf – tPNa	15.7 (12.3–17.7)	15.5 (13.6–17.4)	0.43 [−0.05 to 0.92]	Reference	0.079	0.55 [0.05 to 1.04]	Reference	0.032
t2	25.8 (22.3–28.1)	26.0 (24.2–27.9)	0.12 [−0.43 to 0.67]	Reference	0.663	0.16 [−0.41 to 0.72]	Reference	0.584
t3	36.1 (32.6–39.2)	36.8 (33.4–39.5)	−0.48 [−1.20 to 0.25]	Reference	0.196	−0.24 [−0.99 to 0.51]	Reference	0.528
t4	37.4 (34.5–40.5)	38.2 (35.2–41.0)	−0.44 [−1.17 to 0.30]	Reference	0.240	−0.22 [−0.97 to 0.54]	Reference	0.577
t5	48.8 (43.4–53.4)	49.8 (44.7–54.1)	−1.11 [−2.16 to −0.05]	Reference	0.040	−0.88 [−1.97 to 0.20]	Reference	0.111
t6	51.4 (47.2–55.1)	51.7 (48.0–55.8)	−1.04 [−2.06 to −0.03]	Reference	0.044	−0.81 [−1.86 to 0.25]	Reference	0.133
t7	53.1 (49.3–58.3)	53.5 (49.8–57.9)	−0.46 [−1.55 to 0.62]	Reference	0.402	−0.37 [−1.50 to 0.76]	Reference	0.520
t8	55.2 (51.2–61.5)	55.9 (51.6–61.5)	−0.29 [−1.49 to 0.92]	Reference	0.640	−0.30 [−1.55 to 0.96]	Reference	0.643

Medians are reported in hours (interquartile range). Beta's are reported as estimates in hours for TESE-ICSI embryos to reach a certain time point or interval using ICSI embryos originating from ejaculated sperm as a reference. Model 1: taking clustering of embryos from each couple into account; model 2: taking clustering of embryos from each couple into account and adjusting for the ovarian stimulation approach. A p-value of < 0.05 was considered significant. IQR, interquartile range; tPNa, time between the injection of spermatozoa into the oocyte and appearance of the two pronuclei (PN); tPNf, fading of the PN; tPNf-tPNa, time between tPNa and tPNf; t2, time of cleavage of the embryo to the 2-cell stage; t3, time of cleavage of the embryo to the 3-cell stage; t4, time of cleavage of the embryo to the 4-cell stage; t5, time of cleavage of the embryo to the 5-cell stage; t6, time of cleavage of the embryo to the 6-cell stage; t7, time of cleavage of the embryo to the 7-cell stage; t8, time of cleavage of the embryo to the 8-cell stage.

Table 3. Incidence of embryos showing direct unequal cleavage (DUC) or normal cleavage patterns after TESE-ICSI and ICSI with ejaculated sperm. Pregnancy outcomes after single fresh embryo transfer of all DUC embryos and normal cleaving embryos in the study are presented

	DUC embryos	Normal cleaving embryos	p-value
Fertilization method			
TESE-ICSI	131 (20.5)	508 (79.5)	<0.001
ICSI (with ejaculated sperm)	118 (13.6)	748 (86.4)	
Fetal heartbeat at 12 weeks of gestation			
1	7 (15.6)	129 (39.7)	0.002
2	0 (0)	1 (0.3)	
0	38 (84.4)	195 (60.0)	
Live birth rate			
Singleton	4 (8.9)	99 (30.5)	0.001
Still pregnant during analysis	0 (0)	23 (7.1)	

Data are presented as number (%). A p-value of < 0.05 was considered significant. DUC, direct unequal cleavage (embryos that needed 5 h or less during the interval between the 2- and the 3-cell stage); TESE-ICSI, testicular sperm extraction with intracytoplasmic sperm injection; ICSI, intracytoplasmic sperm injection.

Discussion

Our study showed an earlier pronuclear appearance in TESE-ICSI embryos than in ICSI embryos originating from ejaculated sperm, with a subsequent prolonged interval between pronuclear appearance and pronuclear fading. Moreover, we observed that TESE-ICSI embryos proceeded faster through the cleavage divisions to the 5- and the 6-cell stage, but this effect disappeared when we adjusted our model to take the impact of the ovarian stimulation regimen into account. In addition, we found more DUC embryos in the TESE-ICSI group.

Our observation on faster pronuclear appearance is in line with earlier observations [36, 37]. Sperm DNA damage needs to be repaired in the oocyte after fertilization [22, 23]. If testicular spermatozoa exhibit a lower amount of DNA damage than ejaculated spermatozoa, the oocytes injected with testicular spermatozoa may have less DNA damage to repair. This could potentially enable a

faster transition to pronuclear formation [18]. However, reported differences in DNA damage between testicular and ejaculated sperm are based on samples of normo- and oligozoospermic men, whether these results are generalizable to azoospermic men is unclear. We also observed that after faster pronuclear appearance, TESE-ICSI embryos needed more time before pronuclear envelope breakdown. In mice, severe levels of paternal DNA damage result in a delay of DNA replication in the paternal pronucleus, whereas the maternal pronucleus waits until pronuclear membrane breakdown can proceed synchronously [51]. Although delayed pronuclear fading due to DNA damage and repair would be consistent with our time-lapse observations, it is not consistent with the reported lower incidence of DNA damage in testicular sperm vs ejaculated sperm. We also did not observe a difference in timing of pronuclear fading in NOA and OA testicular sperm-derived embryos, whereas sperm DNA fragmentation has been reported to be higher in testicular sperm from NOA than from OA cases [52]. However, a higher incidence in severe DNA damage could explain the lower fertilization rate in NOA cases than in OA cases, as observed by us and others [48–50].

Alternatively, sperm chromatin structure may also impact pronuclear development. The chromatin of testicular sperm undergoes further compaction during epididymal transit, as the incorporated protamines enfolding the DNA undergo further stabilization by forming S-S bonds [53]. Indications exist in mouse that the histone-to-protamine transition may be incomplete in testicular-derived sperm [54]. Immediately after fertilization, protamines enfolding the DNA in mature sperm cells are replaced with histones H3 and H4 provided by the oocyte. Research in both mouse and human embryos shows that residual histones present in the fertilizing sperm are transmitted to the embryo [55, 56]. This carry-over of histones has been shown in mouse to have an impact on the onset of embryonic gene expression, but it is unknown if and how this phenomenon might affect the formation of the male pronucleus and downstream embryo developmental kinetics [57].

The epididymal epithelium produces exosome vesicles, which are able to transfer RNA molecules to the passing sperm cells [58]. There are indications that sperm RNAs transmit environmental information to the offspring, possibly influencing the phenotype of the offspring [59]. It remains unclear if and what kind of role these RNAs play during early embryo development after fertilization. Conflicting results on this issue were reported. One study concluded that sperm-borne RNAs from within or near the caput epididymis are critical for early embryo development in mice, because embryos derived from sperm originating from the caput epididymis implanted inefficiently and did not develop further [60]. They also showed an effect after fertilization on the expression of a group of RNA and chromatin regulators in the early embryo. However, three other groups did observe normal development of mice after injecting oocytes with sperm from the caput epididymis [61–63]. Thus testicular spermatozoa are likely to have a different content of sperm carried RNAs, but how this may contribute to the differences we observe remain to be identified.

Also in line with previous findings, more TESE-ICSI embryos than ICSI embryos originating from ejaculated sperm showed DUC in our cohort [34]. We observed lower implantation rates of DUC embryos than normal cleaving embryos irrespective of sperm origin, confirming previous findings [47]. The exact cause of DUC is unclear, but it was reported to be associated with maternal genetic variants in a gene region where also the master regulator of centriole duplication, polo-like kinase 4 (PLK4), is located [64]. Centrioles form the core of the centrosome, an organelle that is essential for organizing the microtubules of the mitotic spindle [65]. The number of centrioles is critical for proper chromosome segregation, and, just like chromosomes, their number is reduced during gametogenesis. Supernumerary centrosomes can lead to mitotic spindles with more than two spindle poles and multipolar cell division [66]. In mouse and Drosophila, it was shown that centrosomal components are reduced during spermiogenesis under the regulation of PLK4, and that this is necessary to transmit a functional centrosome to the embryo [67, 68]. In humans, this reduction results in each mature spermatozoon to carry two remodeled centrioles that combine with proteins provided by the oocyte into a reconstituted centrosome in the zygote [69]. It was recently shown in mouse that the centrosome reduction process is not completed as sperm cells leave the testis, but continues during transit through the epididymis [70]. Interestingly, investigations in the domestic cat demonstrated differences in the ability of the sperm centrosome to contribute to sperm aster formation in the zygote, when centrosomes from testicular spermatozoa were compared to those from ejaculated spermatozoa [71]. The testicular sperm centrosome gave rise to poor quality aster formation, which was also associated with a delayed first cleavage. Thus, we hypothesize that the higher incidence of DUC embryos we observe in our study is the result of testicular spermatozoa carrying insufficiently reduced or matured centrioles to the oocyte. This could likely lead to multipolar spindle formation, but it may also affect the duration of the first cell cycle. Recently, novel morphokinetic events were identified using time-lapse imaging of human embryos, among which the appearance of a cytoplasmic wave occurring shortly before PN appearance [72]. It was hypothesized that this is the morphokinetic manifestation of the formation of the microtubule sperm aster, emanating from the centrosome. Although consistently observed to appear shortly before PN appearance in regular ICSI embryos, it would be interesting to investigate this phenomenon in TESE-ICSI embryos in relation to earlier PN formation and DUC.

The reduced implantation rate of DUC embryos might be explained by a more pronounced or different molecular inhomogeneity of the cytoplasmic composition of the resulting blastomeres. It is proposed that inhomogeneity is regulated by intracellular compartmentalization, and unequal cleavage might distribute these compartments different between the resulting three blastomeres [73]. This could lead to biological consequences, since cell fate decisions beyond the 8-cell stage can be influenced by molecules inherited from previous divisions [73].

TESE-ICSI embryos appeared to undergo the subsequent cleavage divisions to the 5- and the 6-cell stage faster, but this effect disappeared when we adjusted for the type of ovarian stimulation regimen used. In our cohort, more women in the TESE-ICSI group underwent ovarian stimulation using GnRH-agonist co-treatment. The choice of ovarian stimulation regimen is standardized in our clinic and is not assigned based on patient characteristics. Recent work investigating the impact of male factor infertility on morphokinetics of embryos resulting from ICSI with ejaculated sperm or routine IVF, reported to find no effect on the duration of the cleavage divisions and time to blastulation after controlling for female factors [74]. These findings suggest that the dynamics of the cleavage divisions are mainly controlled by the oocyte and factors impacting on oocyte quality. Consistent with this, we also did not observe a difference in embryo developmental kinetics, when comparing embryos resulting from ejaculated sperm with or without severe oligoasthenozoospermia. An important female characteristic known to impact IVF outcomes, female age, was comparable between the TESE-ICSI and ICSI with ejaculated sperm group in our study population. However,

we did not study endocrine indicators of ovarian aging and oocyte quality.

Our study included, to our knowledge, the largest cohort of TESE-ICSI embryos studied by time-lapse imaging. Culture conditions were the same during the entire study period and all annotations were performed by the same four team members, resulting in close inter-observer agreement of annotations. However, we do acknowledge the limitation of the retrospective and observational nature of this study. Also, ejaculated sperm was used fresh after selection through density centrifugation, whereas testicular sperm in our study was frozen and thawed. Density centrifugation has been described to select sperm with lower levels of DNA damage [75]. Cryopreservation on the other hand has been described to induce DNA fragmentation, especially in sperm with susceptible, less condensed, chromatin [76–78]. However, there are indications that no differences exist in DNA damage between a fresh and cryopreserved testicular sample. A previous study did not observe a significant increase in testicular sperm DNA fragmentation after cryopreservation, when comparing samples from patients that did and did not undergo cryopreservation. They also reported no differences in treatment outcome when comparing the use of fresh or frozen–thawed testicular sperm [79]. Another study did not observe a significant difference in DNA damage, when comparing a fresh and cryopreserved testicular sample from the same patient [80]. Furthermore, another study comparing ICSI embryos originating from either fresh or frozen ejaculated sperm showed no differences in time-lapse morphokinetics [81]. Whether this finding is generalizable to testicular sperm is unclear. We were unable to assess DNA damage before and after freezing in our cohorts of spermatozoa, and we therefore cannot rule out an effect of the sperm cryopreservation procedure on our findings. Still, our observations are clinically relevant as using frozen–thawed TESE samples are common practice in IVF clinics worldwide. This avoids multiple testicular surgeries and no differences were shown in fertilization rate and clinical pregnancy rate between cycles using fresh or frozen–thawed testicular sperm [82, 83].

In conclusion, the pronuclear stage starts earlier and takes longer in TESE-ICSI embryos than in ICSI embryos originating from ejaculated sperm. We were able to confirm the finding of an earlier pronuclear appearance and a higher incidence of DUC in TESE-ICSI embryos. This shows that it is particularly useful to culture TESE-ICSI embryos in a time-lapse incubator, as in this way the transfer of DUC embryos, known to have lower implantation potential, can be avoided. Our findings provide leads to identify the underlying biological mechanisms for the observed differences. Further research should therefore focus on differences between testicular sperm and ejaculated sperm in terms of centriole function, DNA damage and chromatin integrity. To enable more insight into the roles each of these mechanisms could play, it would be of interest to investigate at what stage of the first embryonic cell cycle TESE-ICSI embryos are delayed: before, during, or after DNA replication. This may also provide insight into the potential impact on pregnancies conceived after TESE-ICSI.

Funding

This research was funded by the Division of Reproductive Endocrinology and Infertility, Department of Obstetrics and Gynaecology of the Erasmus MC, University Medical Center, Rotterdam, the Netherlands.

Supplementary material

Supplementary material is available at *BIOLRE* online.

Data availability statement

The data underlying this article cannot be shared publicly because of the privacy of individuals that participated in the study. The data will be shared on reasonable request to the corresponding author.

Author's contributions

E.B. designed the clinical study. E.M., E.B., and J.H. designed the statistical analysis. E.M., E.C., J.H., and E.B. performed the time-lapse annotations. E.M., J.S., W.B., M.D., E.C., and E.B. collected data. E.M., J.S., J.H., R.S.T, J.L., and E.B. analyzed and interpreted the data. E.M. drafted the manuscript. R.S.T., J.L., and E.B. performed critical revision of the manuscript. All authors have given approval for publication of the present version of this manuscript.

Acknowledgments

The authors thank P.J. Duis von Damm and L. van Duijn for their contribution to the data collection.

Conflict of interest

The authors have declared that no conflict of interest exists.

References

1. Devroey P, Liu J, Nagy Z, Tournaye H, Silber SJ, Van Steirteghem AC. Normal fertilization of human oocytes after testicular sperm extraction and intracytoplasmic sperm injection. *Fertil Steril* 1994; **62**:639–641.
2. Silber SJ, Van Steirteghem AC, Liu J, Nagy Z, Tournaye H, Devroey P. High fertilization and pregnancy rate after intracytoplasmic sperm injection with spermatozoa obtained from testicle biopsy. *Hum Reprod* 1995; **10**:148–152.
3. Devroey P, Liu J, Nagy Z, Goossens A, Tournaye H, Camus M, Van Steirteghem A, Silber S. Pregnancies after testicular sperm extraction and intracytoplasmic sperm injection in non-obstructive azoospermia. *Hum Reprod* 1995; **10**:1457–1460.
4. Charny C. Testicular biopsy its value in male sterility. *JAMA* 1940; **115**:1429–1433.
5. Vloeberghs V, Verheyen G, Haentjens P, Goossens A, Polyzos NP, Tournaye H. How successful is TESE-ICSI in couples with non-obstructive azoospermia? *Hum Reprod* 2015; **30**:1790–1796.
6. Halpern JA, Brannigan RE, Schlegel PN. Fertility-enhancing male reproductive surgery: glimpses into the past and thoughts for the future. *Fertil Steril* 2019; **112**:426–437.
7. Donoso P, Tournaye H, Devroey P. Which is the best sperm retrieval technique for non-obstructive azoospermia? A systematic review. *Hum Reprod Update* 2007; **13**:539–549.
8. ASRM PC. The management of obstructive azoospermia: a committee opinion. *Fertil Steril* 2019; **111**:873–880.
9. Silber S, Escudero T, Lenahan K, Abdelhadi I, Kilani Z, Munne S. Chromosomal abnormalities in embryos derived from testicular sperm extraction. *Fertil Steril* 2003; **79**:30–38.
10. Kahraman S, Sahin Y, Yelke H, Kumtepe Y, Tufekci MA, Yapan CC, Yesil M, Cetinkaya M. High rates of aneuploidy, mosaicism and abnormal morphokinetic development in cases with low sperm concentration. *J Assist Reprod Genet* 2020; **37**:629–640.

11. Kawwass JF, Chang J, Boulet SL, Nangia A, Mehta A, Kissin DM. Surgically acquired sperm use for assisted reproductive technology: trends and perinatal outcomes, USA, 2004-2015. *J Assist Reprod Genet* 2018; **35**:1229–1237.
12. Gervasi MG, Visconti PE. Molecular changes and signaling events occurring in spermatozoa during epididymal maturation. *Andrology* 2017; **5**:204–218.
13. Schoysman R, Vanderzwalmen P, Nijs M, Segal-Bertin G, van de Casseye M. Successful fertilization by testicular spermatozoa in an in-vitro fertilization programme. *Hum Reprod* 1993; **8**:1339–1340.
14. Craft I, Bennett V, Nicholson N. Fertilising ability of testicular spermatozoa. *Lancet* 1993; **342**:864.
15. Tournaye H, Camus M, Goossens A, Liu J, Nagy P, Silber S, Van Steirteghem AC, Devroey P. Recent concepts in the management of infertility because of non-obstructive azoospermia. *Hum Reprod* 1995; **10**:115–119.
16. Sullivan R, Mieusset R. The human epididymis: its function in sperm maturation. *Hum Reprod Update* 2016; **22**:574–587.
17. Haidl G, Badura B, Schill WB. Function of human epididymal spermatozoa. *J Androl* 1994; **15**:23S–27S.
18. Esteves SC, Roque M, Bradley CK, Garrido N. Reproductive outcomes of testicular versus ejaculated sperm for intracytoplasmic sperm injection among men with high levels of DNA fragmentation in semen: systematic review and meta-analysis. *Fertil Steril* 2017; **108**:456–467 e1.
19. Vojtech L, Woo S, Hughes S, Levy C, Ballweber L, Sauteraud RP, Strobl J, Westerberg K, Gottardo R, Tewari M, Hladik F. Exosomes in human semen carry a distinctive repertoire of small non-coding RNAs with potential regulatory functions. *Nucleic Acids Res* 2014; **42**:7290–7304.
20. Cave T, Desmarais R, Lacombe-Burgoyne C, Boissonneault G. Genetic instability and chromatin remodeling in spermatids. *Genes (Basel)* 2019; **10**:40.
21. Ward WS, Coffey DS. DNA packaging and organization in mammalian spermatozoa: comparison with somatic cells. *Biol Reprod* 1991; **44**:569–574.
22. Ahmed EA, Scherthan H, de Rooij DG. DNA double strand break response and limited repair capacity in mouse elongated spermatids. *Int J Mol Sci* 2015; **16**:29923–29935.
23. Derijck A, van der Heijden G, Giele M, Philippens M, de Boer P. DNA double-strand break repair in parental chromatin of mouse zygotes, the first cell cycle as an origin of de novo mutation. *Hum Mol Genet* 2008; **17**:1922–1937.
24. Stringer JM, Winship A, Liew SH, Hutt K. The capacity of oocytes for DNA repair. *Cell Mol Life Sci* 2018; **75**:2777–2792.
25. Fraser R, Lin CJ. Epigenetic reprogramming of the zygote in mice and men: on your marks, get set, go! *Reproduction* 2016; **152**:R211–R222.
26. Rodman TC, Pruslin FH, Hoffmann HP, Allfrey VG. Turnover of basic chromosomal proteins in fertilized eggs: a cytoimmunochemical study of events in vivo. *J Cell Biol* 1981; **90**:351–361.
27. Ciray HN, Aksoy T, Goktas C, Ozturk B, Bahceci M. Time-lapse evaluation of human embryo development in single versus sequential culture media–a sibling oocyte study. *J Assist Reprod Genet* 2012; **29**:891–900.
28. Munoz M, Cruz M, Humaidan P, Garrido N, Perez-Cano I, Meseguer M. Dose of recombinant FSH and oestradiol concentration on day of HCG affect embryo development kinetics. *Reprod Biomed Online* 2012; **25**:382–389.
29. Bellver J, Mifsud A, Grau N, Privitera L, Meseguer M. Similar morphokinetic patterns in embryos derived from obese and normoweight infertile women: a time-lapse study. *Hum Reprod* 2013; **28**:794–800.
30. Cruz M, Garrido N, Gadea B, Munoz M, Perez-Cano I, Meseguer M. Oocyte insemination techniques are related to alterations of embryo developmental timing in an oocyte donation model. *Reprod Biomed Online* 2013; **27**:367–375.
31. Freour T, Dessolle L, Lammers J, Lattes S, Barriere P. Comparison of embryo morphokinetics after in vitro fertilization-intracytoplasmic sperm injection in smoking and nonsmoking women. *Fertil Steril* 2013; **99**:1944–1950.
32. Kirkegaard K, Hindkjaer JJ, Ingerslev HJ. Effect of oxygen concentration on human embryo development evaluated by time-lapse monitoring. *Fertil Steril* 2013; **99**:738–744 e4.
33. Munoz M, Cruz M, Humaidan P, Garrido N, Perez-Cano I, Meseguer M. The type of GnRH analogue used during controlled ovarian stimulation influences early embryo developmental kinetics: a time-lapse study. *Eur J Obstet Gynecol Reprod Biol* 2013; **168**:167–172.
34. Desai N, Gill P, Tadros NN, Goldberg JM, Sabanegh E, Falcone T. Azoospermia and embryo morphokinetics: testicular sperm-derived embryos exhibit delays in early cell cycle events and increased arrest prior to compaction. *J Assist Reprod Genet* 2018; **35**:1339–1348.
35. Scarselli F, Casciani V, Cursio E, Muzzi S, Colasante A, Gatti S, Greco MC, Greco P, Minasi MG, Greco E. Influence of human sperm origin, testicular or ejaculated, on embryo morphokinetic development. *Andrologia* 2018; **50**:e13061.
36. Buran A, Tulay P, Dayioglu N, Bakircioglu ME, Bahceci M, Irez T. Evaluation of the morphokinetic parameters and development of preimplantation embryos obtained by testicular, epididymal and ejaculate spermatozoa using time-lapse imaging system. *Andrologia* 2019; **51**:e13217.
37. Karavani G, Kan-Tor Y, Schachter-Safrai N, Levitas E, Or Y, Ben-Meir A, Buxboim A, Har-Vardi I. Does sperm origin-ejaculated or testicular-affect embryo morphokinetic parameters? *Andrology* 2020; **9**:632–639.
38. Lammers J, Reignier A, Splingart C, Catteau A, David L, Barriere P, Freour T. Does sperm origin affect embryo morphokinetic parameters? *J Assist Reprod Genet* 2015; **32**:1325–1332.
39. Kirkegaard K, Sundvall L, Erlandsen M, Hindkjaer JJ, Knudsen UB, Ingerslev HJ. Timing of human preimplantation embryonic development is confounded by embryo origin. *Hum Reprod* 2016; **31**:324–331.
40. Hoek J, Boellaard WPA, van Marion ES, Willemsen SP, Baart EB, Steegers-Theunissen RPM, Schoenmakers S. The impact of the origin of surgical sperm retrieval on placental and embryonic development: the Rotterdam Periconception cohort. *Andrology* 2020; **9**:599–609.
41. WHO. *WHO Laboratory Manual for the Examination and Processing of Human Semen*, 5th ed. WHO Switzerland; 2010.
42. Eijkemans MJ, Heijnen EM, de Klerk C, Habbema JD, Fauser BC. Comparison of different treatment strategies in IVF with cumulative live birth over a given period of time as the primary end-point: methodological considerations on a randomized controlled non-inferiority trial. *Hum Reprod* 2006; **21**:344–351.
43. de Oliveira NM, Vaca Sanchez R, Rodriguez Fiesta S, Lopez Salgado T, Rodriguez R, Bethencourt JC, Blanes Zamora R. Pregnancy with frozen-thawed and fresh testicular biopsy after motile and immotile sperm microinjection, using the mechanical touch technique to assess viability. *Hum Reprod* 2004; **19**:262–265.
44. Ebner T, Moser M, Shebl O, Sommergruber M, Gaiswinkler U, Tews G. Morphological analysis at compacting stage is a valuable prognostic tool for ICSI patients. *Reprod Biomed Online* 2009; **18**:61–66.
45. Alpha Scientists in Reproductive, M. and E.S.I.G.o. Embryology. The Istanbul consensus workshop on embryo assessment: proceedings of an expert meeting. *Hum Reprod* 2011; **26**:1270–1283.
46. Ciray HN, Campbell A, Agerholm IE, Aguilar J, Chamayou S, Esbert M, Sayed S, G. Time-Lapse User. Proposed guidelines on the nomenclature and annotation of dynamic human embryo monitoring by a time-lapse user group. *Hum Reprod* 2014; **29**:2650–2660.
47. Rubio I, Kuhlmann R, Agerholm I, Kirk J, Herrero J, Escriba MJ, Bellver J, Meseguer M. Limited implantation success of direct-cleaved human zygotes: a time-lapse study. *Fertil Steril* 2012; **98**:1458–1463.
48. De Croo I, Van der Elst J, Everaert K, De Sutter P, Dhont M. Fertilization, pregnancy and embryo implantation rates after ICSI in cases of obstructive and non-obstructive azoospermia. *Hum Reprod* 2000; **15**:1383–1388.
49. Vernaeve V, Tournaye H, Osmanagaoglu K, Verheyen G, Van Steirteghem A, Devroey P. Intracytoplasmic sperm injection with testicular spermatozoa is less successful in men with nonobstructive azoospermia than in men with obstructive azoospermia. *Fertil Steril* 2003; **79**:529–533.

50. Palermo GD, Schlegel PN, Hariprashad JJ, Ergun B, Mielnik A, Zaninovic N, Veeck LL, Rosenwaks Z. Fertilization and pregnancy outcome with intracytoplasmic sperm injection for azoospermic men. *Hum Reprod* 1999; **14**:741–748.
51. Gawecka JE, Marh J, Ortega M, Yamauchi Y, Ward MA, Ward WS. Mouse zygotes respond to severe sperm DNA damage by delaying paternal DNA replication and embryonic development. *PLoS One* 2013; **8**:e56385.
52. Meseguer M, Santiso R, Garrido N, Gil-Salom M, Remohi J, Fernandez JL. Sperm DNA fragmentation levels in testicular sperm samples from azoospermic males as assessed by the sperm chromatin dispersion (SCD) test. *Fertil Steril* 2009; **92**:1638–1645.
53. Saowaros W, Panyim S. The formation of disulfide bonds in human protamines during sperm maturation. *Experientia* 1979; **35**:191–192.
54. Yoshida K, Muratani M, Araki H, Miura F, Suzuki T, Dohmae N, Katou Y, Shirahige K, Ito T, Ishii S. Mapping of histone-binding sites in histone replacement-completed spermatozoa. *Nat Commun* 2018; **9**:3885.
55. van de Werken C, van der Heijden GW, Eleveld C, Teeuwssen M, Albert M, Baarends WM, Laven JS, Peters AH, Baart EB. Paternal heterochromatin formation in human embryos is H3K9/HP1 directed and primed by sperm-derived histone modifications. *Nat Commun* 2014; **5**:5868.
56. van der Heijden GW, Derijck AA, Posfai E, Giele M, Pelczar P, Ramos L, Wansink DG, van der Vlag J, Peters AH, de Boer P. Chromosome-wide nucleosome replacement and H3.3 incorporation during mammalian meiotic sex chromosome inactivation. *Nat Genet* 2007; **39**:251–258.
57. Federici F, Magaraki A, Wassenaar E, van Veen-Buurman CJ, van de Werken C, Baart EB, Laven JS, Grootegoed JA, Gribnau J, Baarends WM. Round spermatid injection rescues female lethality of a paternally inherited Xist deletion in mouse. *PLoS Genet* 2016; **12**:e1006358.
58. Sharma U. Paternal contributions to offspring health: role of sperm small RNAs in intergenerational transmission of epigenetic information. *Front Cell Dev Biol* 2019; **7**:215.
59. Zhang Y, Shi J, Rassoulzadegan M, Tuorto F, Chen Q. Sperm RNA code programmes the metabolic health of offspring. *Nat Rev Endocrinol* 2019; **15**:489–498.
60. Conine CC, Sun F, Song L, Rivera-Perez JA, Rando OJ. Small RNAs gained during epididymal transit of sperm are essential for embryonic development in mice. *Dev Cell* 2018; **46**:470–480 e3.
61. Zhou D, Suzuki T, Asami M, Perry ACF. Caput epididymidal mouse sperm support full development. *Dev Cell* 2019; **50**:5–6.
62. Wang Y, Yamauchi Y, Wang Z, Zheng H, Yanagimachi R, Ward MA, Yan W. Both cauda and caput epididymal sperm are capable of supporting full-term development in FVB and CD-1 mice. *Dev Cell* 2020; **55**:675–676.
63. Fernandez-Gonzalez R, Laguna R, Ramos-Ibeas P, Pericuesta E, Alcalde-Lopez V, Perez-Cerezales S, Gutierrez-Adan A. Successful ICSI in mice using caput epididymal spermatozoa. *Front Cell Dev Biol* 2019; **7**:346.
64. McCoy RC, Newnham LJ, Ottolini CS, Hoffmann ER, Chatzimeletiou K, Cornejo OE, Zhan Q, Zaninovic N, Rosenwaks Z, Petrov DA, Demko ZP, Sigurjonsson S et al. Tripolar chromosome segregation drives the association between maternal genotype at variants spanning PLK4 and aneuploidy in human preimplantation embryos. *Hum Mol Genet* 2018; **27**:2573–2585.
65. Fu J, Hagan IM, Glover DM. The centrosome and its duplication cycle. *Cold Spring Harb Perspect Biol* 2015; **7**:a015800.
66. Ganem NJ, Godinho SA, Pellman D. A mechanism linking extra centrosomes to chromosomal instability. *Nature* 2009; **460**:278–282.
67. Avidor-Reiss T, Mazur M, Fishman EL, Sindhwani P. The role of sperm centrioles in human reproduction-the known and the unknown. *Front Cell Dev Biol* 2019; **7**:188.
68. Khire A, Vizuet AA, Davila E, Avidor-Reiss T. Asterless reduction during spermiogenesis is regulated by Plk4 and is essential for zygote development in drosophila. *Curr Biol* 2015; **25**:2956–2963.
69. Sathananthan AH. Paternal centrosomal dynamics in early human development and infertility. *J Assist Reprod Genet* 1998; **15**:129–139.
70. Simerly C, Castro C, Hartnett C, Lin CC, Sukhwani M, Orwig K, Schatten G. Post-testicular sperm maturation: centriole pairs, found in upper epididymis, are destroyed prior to sperm's release at ejaculation. *Sci Rep* 2016; **6**:31816.
71. Comizzoli P, Wildt DE, Pukazhenthi BS. Poor centrosomal function of cat testicular spermatozoa impairs embryo development in vitro after intracytoplasmic sperm injection. *Biol Reprod* 2006; **75**:252–260.
72. Coticchio G, Mignini Renzini M, Novara PV, Lain M, De Ponti E, Turchi D, Fadini R, Dal Canto M. Focused time-lapse analysis reveals novel aspects of human fertilization and suggests new parameters of embryo viability. *Hum Reprod* 2018; **33**:23–31.
73. Chen Q, Shi J, Tao Y, Zernicka-Goetz M. Tracing the origin of heterogeneity and symmetry breaking in the early mammalian embryo. *Nat Commun* 2018; **9**:1819.
74. Sacha CR, Dimitriadis I, Christou G, James K, Brock ML, Rice ST, Bhowmick P, Bormann CL, Souter I. The impact of male factor infertility on early and late morphokinetic parameters: a retrospective analysis of 4126 time-lapse monitored embryos. *Hum Reprod* 2020; **35**: 24–31.
75. Van Kooij RJ, de Boer P, De Vreeden-Elbertse JM, Ganga NA, Singh N, Te Velde ER. The neutral comet assay detects double strand DNA damage in selected and unselected human spermatozoa of normospermic donors. *Int J Androl* 2004; **27**:140–146.
76. Paoli D, Pelloni M, Lenzi A, Lombardo F. Cryopreservation of sperm: effects on chromatin and strategies to prevent them. *Adv Exp Med Biol* 2019; **1166**:149–167.
77. Cankut S, Dinc T, Cincik M, Ozturk G, Selam B. Evaluation of sperm DNA fragmentation via halosperm technique and TUNEL assay before and after cryopreservation. *Reprod Sci* 2019; **26**:1575–1581.
78. Le MT, Nguyen TTT, Nguyen TT, Nguyen TV, Nguyen TAT, Nguyen QHV, Cao TN. Does conventional freezing affect sperm DNA fragmentation? *Clin Exp Reprod Med* 2019; **46**:67–75.
79. Thompson-Cree ME, McClure N, Donnelly ET, Steele KE, Lewis SE. Effects of cryopreservation on testicular sperm nuclear DNA fragmentation and its relationship with assisted conception outcome following ICSI with testicular spermatozoa. *Reprod Biomed Online* 2003; **7**: 449–455.
80. Steele EK, McClure N, Lewis SE. Comparison of the effects of two methods of cryopreservation on testicular sperm DNA. *Fertil Steril* 2000; **74**:450–453.
81. Eastick J, Venetis C, Cooke S, Storr A, Susetio D, Chapman M. Is early embryo development as observed by time-lapse microscopy dependent on whether fresh or frozen sperm was used for ICSI? A cohort study. *J Assist Reprod Genet* 2017; **34**:733–740.
82. Ohlander S, Hotaling J, Kirshenbaum E, Niederberger C, Eisenberg ML. Impact of fresh versus cryopreserved testicular sperm upon intracytoplasmic sperm injection pregnancy outcomes in men with azoospermia due to spermatogenic dysfunction: a meta-analysis. *Fertil Steril* 2014; **101**:344–349.
83. Yu Z, Wei Z, Yang J, Wang T, Jiang H, Li H, Tang Z, Wang S, Liu J. Comparison of intracytoplasmic sperm injection outcome with fresh versus frozen-thawed testicular sperm in men with nonobstructive azoospermia: a systematic review and meta-analysis. *J Assist Reprod Genet* 2018; **35**:1247–1257.